Hindawi
Journal of Sensors
Volume 2019, Article ID 9512190, 8 pages
https://doi.org/10.1155/2019/9512190

Research Article

Effect of Tensile Force on Magnetostrictive Sensors for Generating and Receiving Longitudinal Mode Guided Waves in Steel Wires

Jiang Xu, Yong Li, and Guang Chen

School of Mechanical Science and Engineering, Huazhong University of Science and Technology, 1037 Luoyu Road, Wuhan, China

Correspondence should be addressed to Jiang Xu; jiangxu@mail.hust.edu.cn

Received 6 August 2018; Revised 19 October 2018; Accepted 22 November 2018; Published 14 February 2019

Academic Editor: Alfredo Guemes

When the longitudinal mode guided waves based on magnetostrictive effect were employed to inspect the bridge cables, we found that there was a large difference in the signal's amplitude of the same specification cable under different tensile force. This difference would affect the test results and the identification of defects. It is necessary to study the effect of tensile force on the signal for the reliability of detection. Firstly, the effective field theory is employed to take the force as an additional bias magnetic field. Then, the effect of the tensile force on generating and receiving longitudinal mode guided waves based on magnetostrictive effect is obtained by the relationship between the bias magnetic field and the magnetostrictive coupling coefficient. Finally, the experiment of the magnetostrictive sensor is carried out on a Φ5 mm steel wire under different force. The experimental results are in good agreement with the theoretical results. The results show that the existence of the tensile force would change the operation point for generating and receiving the longitudinal mode guided waves based on magnetostrictive effect, which associated with the coupling coefficient. In order to obtain the optimal conversion efficiency for the force state wire and cable, the applied bias magnetic field should be set smaller than the bias magnetic field for the force-free state.

1. Introduction

Cables are widely used in the bridge construction, such as cable-stayed bridges, concrete-filled steel tube arch bridges, and suspension bridges [1]. As the main tension element of these bridges, the damage of the cables will lead to the decline of the load carrying capacity of the bridge. More seriously, the broken cables would cause the collapse accident of the bridges, such as Kongquehe Bridge in China and Mahakam II Bridge in Indonesia. Recently, the longitudinal mode guided wave technology based on the magnetostrictive effect was employed to inspect the bridge cables which could achieve long-range detection from one point [2–8]. Guided wave testing using the magnetostrictive sensors includes the wave excitation and reception, based on magnetostrictive effect and its invert effect. The energy coupling coefficient of the sensors is concerned with the magnetization state of the ferromagnetic components which is determined by the superimposed magnetization of the static bias magnetic field and the alternating magnetic field. The bias magnetic field provides an operating point in the magnetostrictive curve [9]. The engineers tend to set the bias magnetic field to the optimal operating point which corresponds to the maximum coupling efficiency to improve sensitivity.

The initial tensile force was set to the design value [1]. However, the force would adjust itself according to the balance of the bridge after many years of service. The force appeared as a stress in the wires, and the change of tension had an influence on the amplitude of the magnetostrictive guided wave testing signal. In many bridge inspection projects, we found that there was a large difference in signal amplitude when the transducer's parameters were the same for the same specification cables. Since the signal amplitude would affect the assessment of defects, it is necessary to study the influence of the force on magnetostrictive sensors for generating and receiving longitudinal mode guided waves in steel wires. The existing studies mainly focused on two aspects. On the one hand, the influence of tensile force on the propagation characteristics of guided waves was studied [10–18]. These features such as the notch frequency, the higher order group velocity, and the relative velocity variation could be employed to measure the force.

On the other hand, the influence of tension on the magnetization state was studied, such as the magnetoelastic model [19–22]. However, little research has been done on the effect of the tensile force on the coupling efficiency of magnetostrictive sensors [23–25].

The aim of this paper is to study the effect of the tensile force on magnetostrictive guided wave sensors and provide support for compensating the testing signal. The influence of the force applied to guided wave testing includes three parts. The first part is the influence of the force for generating guided waves. The second part is the influence of the force to the propagation of guided waves. The third part is the influence of the force for receiving guided waves. To study the first part and the third part, the equivalent relationship between the force and the bias magnetic field is analyzed based on the principle of magnetostrictive effect and the effective field theory. To reduce the wave propagation effect, the attenuation coefficient of the guided wave in the steel wire is employed to compensate the signal. Then, the influence of the tensile force on the coupling coefficient is studied using the relationship between the bias magnetic field and the magnetostrictive coupling coefficient. Finally, the experiments are carried out on a 5 mm steel wire with different force. The experimental results are compared with the theoretical results. Since the tensile force can be taken as an additional magnetic field to the bias magnetic field, the force has similar effect as the bias magnetic field on the coupling coefficient.

2. Principle

2.1. The Principle of Magnetostrictive Guided Wave Sensor. The sensor for detecting steel wires is based on the magnetostrictive effect and its inverse effect. In general, the magnetostrictive constitutive equations can be expressed as

$$\varepsilon = s^H \sigma + dH, \tag{1}$$

$$B = d' \sigma + \mu^\sigma H, \tag{2}$$

where ε and σ are the strain and the stress, respectively, H is the magnetic field strength, s^H is the elastic compliance matrix caused by H, μ^σ is the magnetic permeability matrix under constant stress, B is the magnetic flux density, d is the magnetostrictive matrix and $'$ is the matrix transpose. Equation (1) is the magnetostrictive effect in which strain is generated by magnetic field, and equation (2) is the inverse effect in which magnetic flux is generated by stress.

For wave generating, when the wire is subjected to the superimposed magnetization of the bias magnetic field and the alternating magnetic field, the corresponding parts of the wire will generate axial vibrations. The vibrations propagate along the wire in the form of mechanical waves. For wave receiving, when the mechanical waves reach the position of the receiving coil, the mechanical vibrations under the bias magnetic field cause the magnetic flux variations, which lead to the receiving coil generating the electrical signal. The position and size information of the defect can be obtained by analyzing the receiving signal. The schematic diagram of magnetostrictive guided wave technology for detecting steel wires is shown in Figure 1.

2.2. The Relationship between the Bias Magnetic Field and the Magnetostrictive Guided Wave Coupling Coefficient. The magnetostrictive guided wave coupling coefficient is closely related to the bias magnetic field. Many scientists have studied this problem [26–29]. The model of the magnetostrictive longitudinal guided wave excitation process can be expressed as [20, 30]

$$h_\lambda(M) = -\frac{1}{2}\left(3\widehat{\lambda} + 2\widehat{\mu}\right)(1-2\nu)\frac{\partial \lambda}{\partial M_0}, \tag{3}$$

where $h_\lambda(M)$ is the coupling constant, M is the magnetization intensity, λ is the magnetostrictive coefficient, $\widehat{\lambda}$ and $\widehat{\mu}$ are the Lame constant, ν is the Poisson coefficient, and M_0 is the static bias magnetic field strength. In equation (3), the excitation coupling coefficient of magnetostrictive guided waves is proportional to the derivative of the magnetostrictive coefficient and not to the magnetostrictive coefficient itself. The magnetostrictive coefficient is determined by the bias magnetic field strength, so the bias magnetic field directly affects the coupling coefficient.

For the receiving process, the bias magnetic field also has an influence on the coupling coefficient. When the bias magnetic field is much greater than the dynamic magnetic field, the rate of the magnetization change over time can be expressed as [21]

$$\frac{dM}{dt} = \frac{\partial M_s(Coth(H/a) - a/H)}{\partial \sigma}\frac{\partial \sigma}{\partial t}, \tag{4}$$

where M_s is the saturation magnetization, a is the magnetic domain density, and t is the time. Equation (4) shows that the bias magnetic field strength affects the receiver signal amplitude.

From the above analysis, it can be seen that coupling coefficient of guided wave excitation and receiving process are closely related to the bias magnetic field. Since the excitation and receiving process of the magnetostrictive longitudinal guided waves are reciprocal process, the impacts of force on magnetostrictive effect and its inverse effect are similar. Based on the Le Chatelier's principle, it can be expressed as

$$\left.\frac{\partial \varepsilon}{\partial H}\right|_\sigma = \left.\frac{\partial B}{\partial \sigma}\right|_H. \tag{5}$$

The left side of equation (5) is the rate of change of magnetostrictive strain with magnetic field under constant stress, which is used to characterize the magnetostrictive effect. The right side of equation (5) is the rate of change of the magnetic induction intensity with the stress, which is used to characterize the inverse magnetostrictive effect.

2.3. Effective Field Theory. J-A (Jiles-Atherton) model is based on the magnetic domain theory of ferromagnetic materials to describe the relationship between magnetic field strength and magnetic induction. However, the J-A model

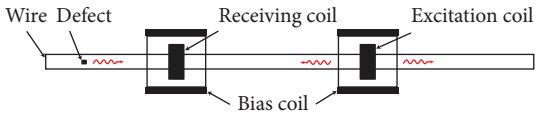

Figure 1: Schematic diagram of magnetostrictive sensors for steel wires.

is a one-dimensional model, which cannot be applied to the case of anisotropy. Sablik et al. proposed J-A-S (Jiles-Atherton-Sablik) model to deal with the stress field [21, 31–33]. In J-A-S model, a magnetic field strength component H_σ due to the stress is added to the J-A model. This model can be more effective to explain the magneto-mechanical coupling phenomenon. Based on J-A-S model, the effective field can be expressed as

$$H_e = H + \alpha M + H_\sigma, \tag{6}$$

where α is a dimensionless mean field parameter and H_σ is a term added here to account for stress contribution to the effective field.

The field H_σ has to change sign with magnetization and hence is an odd power of the magnetization. It is suggested that a linear combination of terms in M and M^3 would be even better. H_σ is expressed as [31]

$$H_\sigma = \frac{3}{2}\left(\frac{\sigma}{\mu_0 M_s}\right)\left\{\frac{M}{M_s}\left[\lambda_1 + \frac{3}{2}\lambda_3\left(\frac{M}{M_s}\right)^3\right]\right\}, \tag{7}$$

where μ_0 is the magnetic permeability in air and λ_1 and λ_3 are coefficients related to the magnetostrictive properties of the component.

2.4. Effect of Tensile Force on Coupling Coefficient of Magnetostrictive Guided Waves. For generating and receiving guided wave based on magnetostrictive effect, the corresponding section of wire should be magnetized to near saturation. When the wire is subjected to tension, the stress would act as an additional bias magnetic field which leads to an increase in the bias magnetic field according to equation (6). Because the initial value of the bias magnetic field H and the magnetization M can be obtained by experiments, the effective field H_e caused by stress can be obtained by equation (7). The operation point of the sensor would change with the increase of the bias magnetic field. Taking the excitation process as an example, according to the derivative chain rule (8), equation (3) can be deduced as equation (9).

$$\frac{d\lambda}{dM} = \frac{\partial\lambda}{\partial H}\frac{\partial H}{\partial M}, \tag{8}$$

$$h_\lambda(M)|_{He} = --\frac{1}{2(\mu_r - 1)}\left(3\widehat{\lambda} + 2\widehat{\mu}\right)(1 - 2\nu)\left.\frac{\partial\lambda}{\partial H}\right|_{He}. \tag{9}$$

In equation (9), the coupling coefficient of the magnetostrictive guided wave excitation process is related to the derivative of the magnetostrictive coefficient $\partial\lambda/\partial H$ and the relative magnetic permeability μ_r. We can obtain the relationship between the magnetic field strength H and the excitation coupling coefficient by experiments. Similarly, the relationship between the receiving coupling coefficient and the bias magnetic field can also be obtained by experiments. The steps to estimate the theoretical results are as follows:

(1) Firstly, the initial value of the bias magnetic field H, the B-H curve of the wire, and the excitation and receiving coupling coefficient curves are obtained by experiments

(2) Secondly, the stress magnetic field (H_σ) is calculated using equation (7)

(3) Thirdly, the effective bias magnetic field (H_e) is calculated using equation (6)

(4) Finally, the relationship between the force and the coupling coefficient is obtained from the excitation and receiving coupling coefficient curves based on the effective bias magnetic field (H_e)

3. Experimental Setup

Experimental measurements of wave generation and reception were made for comparison to the theoretical results. These measurements involved obtaining the *B-H* curve, the excitation and receiving coupling coefficient curves in the steel wire, and recording the data produced in a receiving coil with the increase of the tension. A high-strength steel wire for bridge cables of 5.8 m length, 5 mm diameter, and 1860 MPa ultimate tensile strength was employed for the experiments. The dispersion curves of the wire are shown in Figure 2.

3.1. B-H Curve Experiments. The experiment system for obtaining the magnetization curve is provided in Figure 3 [7]. The magnetizing coil was made of American wire gauge no. 18 enameled wire with 15.3 mm outer diameter, 12.6 mm inner diameter, 626.0 mm length, three layers, and 1740 turns. The measuring coil was made of American wire gauge no. 31 enameled wire with 6.0 mm outer diameter, 5.8 mm inner diameter, 34.0 mm length, single layer, and 150 turns. The input current to the magnetizing coil increased from 0 to 16 A with a step of 0.1 A.

3.2. Excitation and Receiving Coupling Coefficient Curve Experiments. The experiment system for obtaining the excitation and receiving coupling coefficient curve is shown in Figure 4. Additionally, the system could also obtain the relation between the magnetizing current and the longitudinal component of the static bias magnetic field using the Hall probe [27]. The magnetizing coils were made of American wire gauge no. 13 enameled wire with 66 mm outer diameter, 50 mm inner diameter, 178 mm length, five layers, and 500 turns. The transmitting coil and the receiving coil were made of American wire gauge no. 31 enameled wire with 6.0 mm outer diameter, 5.8 mm inner diameter, 26 mm length (about 1/4 wavelength of L(0,1) at 50 kHz), single layer, and 100 turns. A magnetostrictive guided waves inspection system was employed. It consisted of a signal generator, a pulse

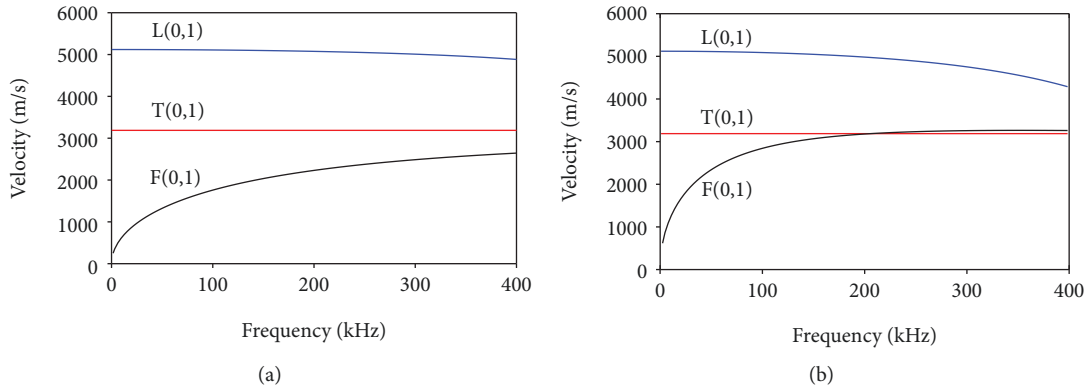

Figure 2: The dispersion curves of the steel wire of 5 mm diameter. (a) Phase speed. (b) Group speed.

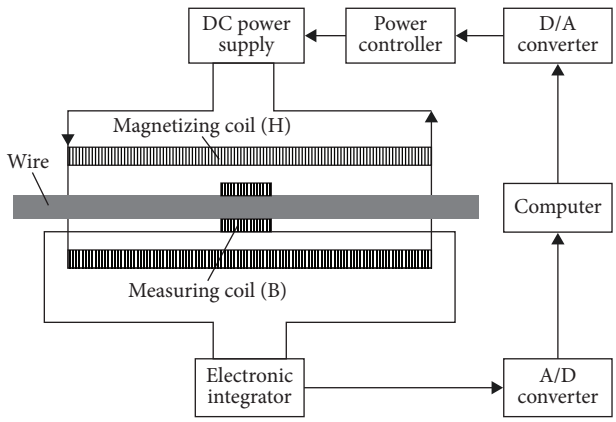

Figure 3: The experimental setup for obtaining the B-H curve of the steel wire.

power amplifier, a preamplifier, an analog-to-digital converter, and a computer. The position of the sensors in the wire is shown in Figure 5 (the receiver at R1 location). To obtain the excitation coupling coefficient curve of the unloaded wire, the input current of the magnetizing coil at the transmitting side increased from 0 to 16 A with a step of 0.5 A and the input current of the magnetizing coil at the receiving side was fixed at 7 A. At each current of the magnetizing coil at the transmitting coil, the Hall probe was employed to acquire the magnetic strength on the surface of the wire, and the computer controlled signal generator to generate a 4-cycle sine wave of Hanning window and the frequency was 50 kHz. The burst was amplified by the power amplifier and then inputted the excitation coil to produce an alternating magnetic field. The input power is about 2 kW. The receiving coil obtained the change of magnetic flux by Faraday's law of induction. The signal was amplified by the preamplifier and then converted to digital signal by analog-to-digital converter. At last, the signal was stored in the computer. Similarly, to obtain the excitation coupling coefficient curve of the unloaded wire, the input current of the magnetizing coil at the receiving side increased from 0 to 16 A with a step of 0.5 A and the input current of the magnetizing coil at the transmitting side was fixed at 7 A.

3.3. Effect of Tensile Force to the Coupling Coefficient of the Magnetostrictive Sensor Experiments. The experiment setup to study the effect of tensile force to the coupling coefficient of the magnetostrictive sensor is shown in Figure 5. The breaking force of the wire is about 3.65 kN. In the experiments, the force increased from 0 to 19.6 kN (1000 MPa) with a step of 0.98 kN (50 MPa). The input current of the magnetizing coil at the transmitting side and the transmitting side were fixed at 7 A. Other parameters were same as Section 3.2.

4. Results and Discussions

4.1. B-H Curve, the Excitation and Receiving Coupling Coefficient Curves. The B-H curve of the wire using the experimental system in Figure 3 is shown in Figure 6. The curves between the input current to the magnetizing coil and the longitudinal component of the static bias magnetic field under unloaded status on the transmitting side and receiving side are shown in Figure 7. The relationship is almost linearity. The initial value of the bias magnetic field H corresponding to a certain bias current could be obtained from the curves.

Using the setup in Section 3.2, the signal at the input current of the magnetizing coil at the transmitting side and receiving side were 7 A obtained from the unloaded wire is shown in Figure 8. The initial pulse induced by the receiving coil was the electromagnetic wave generated by the excitation coil which propagated directly from the air at the speed of light. The first passing signal induced by the receiving coil was the elastic wave generated in the wire by the excitation coil which propagated from the excitation coil position to the receiving coil in the wire. The arrival time of the first passing signal was 0.384 ms. The distance between the excitation coil and the receiving coil was 2000 mm. Therefore, the velocity of the wave was about 5208 m/s. According to the group dispersion curve of the wire, we could ensure that the wave was the first longitudinal mode (L(0,1)) at 50 kHz. The voltage peak-peak value (Vpp) of the first passing signal was employed to represent the magnetostrictive coupling coefficient. To obtain the magnetostrictive coupling coefficient curve at the transmitting side, the input current of the magnetizing coil at the transmitting side increased from 0

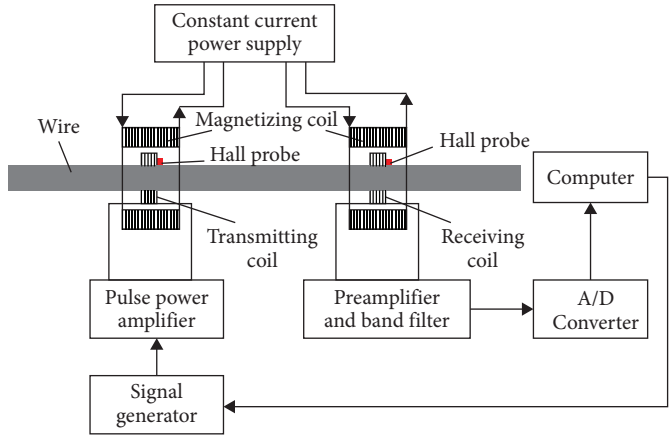

Figure 4: The experimental setup for obtaining the excitation and receiving coupling coefficient curve of the steel wire.

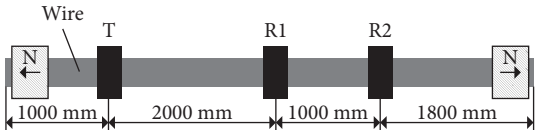

Figure 5: The experiment setup for studying the effect of tensile force to the coupling coefficient. T: transmitter; R1 and R2: the two positions of the receiver; N: tensile force.

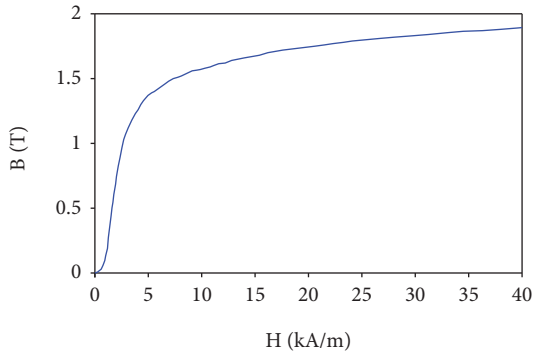

Figure 6: The B-H curve of the steel wire using the experimental system shown in Figure 3.

to 16 A with a step of 0.5 A and the input current of the magnetizing coil at the receiving side was fixed at 7 A. The magnetostrictive coupling coefficient curve at the transmitting side is shown in Figure 9 (blue line). The magnetostrictive coupling coefficient curve at the receiving side is obtained using the similar method as shown in Figure 9 (red line).

4.2. The Relationship between the Stress and the Magnetostrictive Coupling Coefficient. To obtain the theory results, the effective field under different stress should be obtained. Firstly, the initial value of the bias magnetic field H corresponding to 7 A bias current was obtained from the curves shown in Figure 7. The bias magnetic strength at the transmitting side and the receiving side of the unloaded wire were 17.88 kA/m and 17.57 kA/m, respectively. Because the material of the wire is very similar as AISI 410 having Rockwell C Hardness 42, some parameters are $M_s = 1.35 \times 10^3$ kA/m, $\alpha = 0.0033$, $\lambda_1 = 5 \times 10^{-6}$, and $\lambda_3 = 14 \times 10^{-5}$ which is from Ref. [29]. Using equations (6) and (7), the effective bias magnetic field increased from 17.88 kA/m to 36.78 kA/m at the transmitting side and from 17.57 kA/m to 35.64 kA/m at the receiving side when the stress increased form 0 MPa to 1000 MPa. Secondly, the magnetostrictive coupling coefficients corresponding to the effective bias magnetic field at the transmitting side and the receiving side were obtained from Figure 9. The data were normalized by using the magnetostrictive coupling coefficient at the initial value bias magnetic field (0 MPa). Finally, the theoretical curve of the stress and the magnetostrictive coupling coefficient was obtained by multiplying the transmitting coupling coefficient and the receiving coupling coefficient. The results are shown in Figure 10 (blue line).

To reduce the effect of the force applied to the wire on the propagation characteristics of guided waves, the attenuation coefficient was employed to compensate the experimental results. The equation to calculate the attenuation coefficient A_{AC} is as follows:

$$A_{AC} = \frac{20\lg(V_{FPSR2}/V_{FPSR1})}{L}, \quad (10)$$

where V_{FPSR2} is the peak-peak value of the signal received at location R1, V_{FPSR1} is the peak-peak value of the signal received at location R2, and L is the propagation distance of the guided wave (here is 1000 mm).

The relation between the stress and the attenuation coefficient is shown in Figure 11. The results show that the attenuation coefficient had a little change with the increasing of the stress. The attenuation coefficient decreased with the increasing of the stress. The attenuation coefficients were employed to compensate the signal. Then, the receiving signals were normalized by using the unloaded status signal. The relationship between the stress and the normalized receiving signal is shown in Figure 10.

Good agreement is obtained between the experimental and theoretical results as shown in Figure 10. The coupling coefficient increases with the increase of stress when the

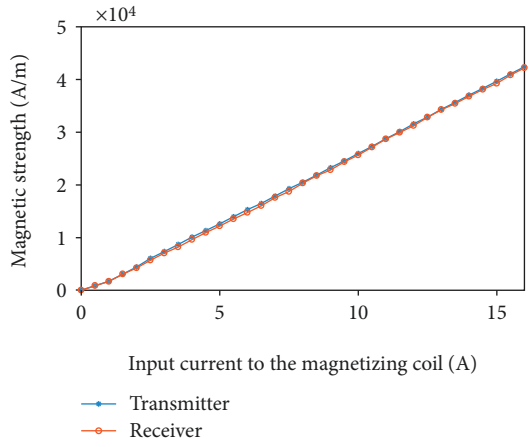

Figure 7: The relation curves between the input current to the magnetizing coil and the longitudinal component of the static bias magnetic field under unloaded status on the transmitting side and receiving side.

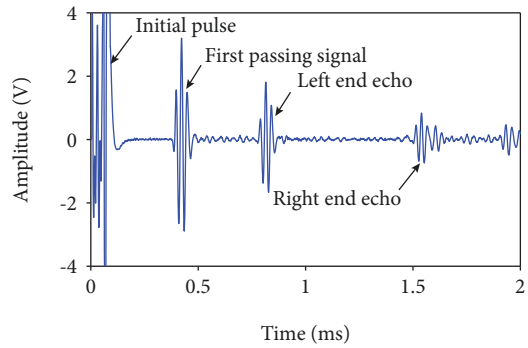

Figure 8: The signal at the input current of the magnetizing coil at the transmitting side and receiving side were 7 A obtained from the unloaded wire using the setup in Section 3.2.

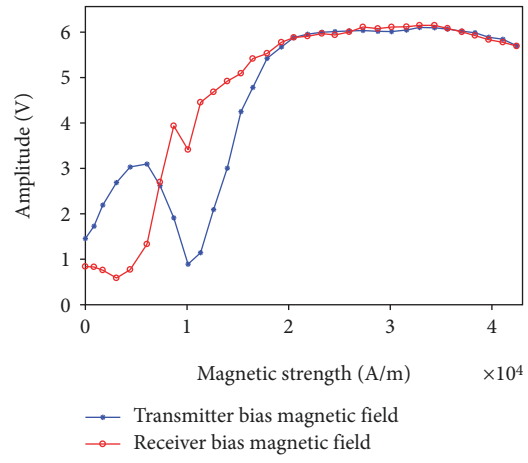

Figure 9: The magnetostrictive coupling coefficient curves at the transmitting side (the current of the magnetizing coil at receiving side is fixed on 7 A) and the receiving side (the current of the magnetizing coil at transmitting side is fixed on 7 A) at the unloaded wire.

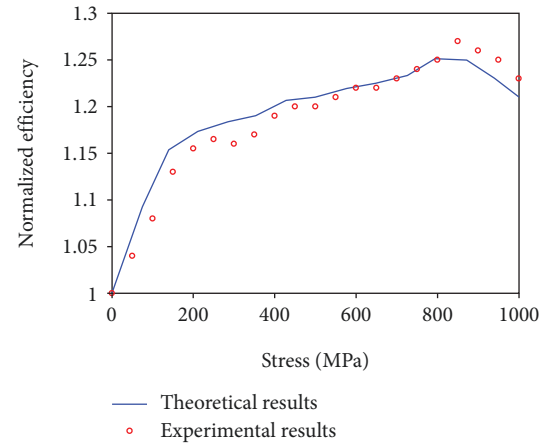

Figure 10: The relationship between the stress and the magnetostrictive coupling coefficient.

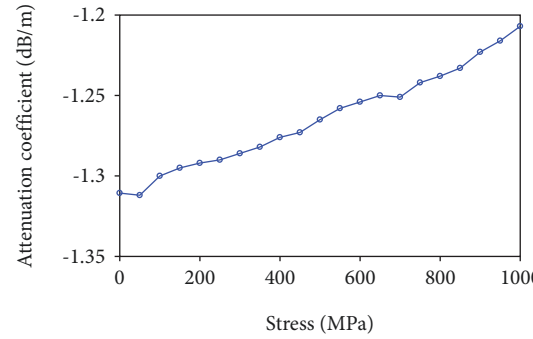

Figure 11: The relation between the stress and the attenuation coefficient.

stress is less than 850 MPa. Then the coupling coefficient decreases with the increase of stress when the stress is larger than 850 MPa. This phenomenon could be explained that the stress provides an additional bias magnetic field in the wire. The additional bias magnetic field changes the operation point of the magnetostrictive sensor which is associated with the coupling coefficient. The effect of the stress on the coupling coefficient can reach about 27% amplitude change. The influence is closely related to the initial bias magnetic field strength. However, there are some estimation errors on the theoretical results and the experimental results, the reason may be from the linear hypothesis between the stress and the effective field. To obtain more precise theoretical results, the relation of the stress and the magnetization intensity should be measured by experiments.

5. Conclusions

In this paper, the effect of tensile force on magnetostrictive sensors for generating and receiving longitudinal mode guided waves in the wire is studied. The effective field theory is employed to take the force account into the bias magnetic field. The results show that the force could be taken as an additional bias magnetic field, which would change the operation point and affect the magnetostrictive coupling

coefficient. The use of magnetostrictive sensor to detect the wires and the cables tends to set the bias magnetic field to the best operating point of the force-free state. However, in order to obtain the optimal conversion efficiency for the force state wire and cable, the applied bias magnetic field should be set smaller than the bias magnetic field for the force-free state. Additionally, it is necessary to consider the effect of tensile force on coupling coefficient and compensate the signal to obtain reliable detection results when wires and cables are under different force conditions in practical application.

Data Availability

The data used to support the findings of this study are included within the article.

Conflicts of Interest

The authors declare that they have no conflicts of interest.

Acknowledgments

This work was supported by the National Natural Science Foundation of China (Grant no. 51575213) and the National Key Research and Development Program of China (Grant no. 2016YFC0801904). The authors acknowledge supports for this work by Jiangsu Fasten Steel Cable Co. Ltd.

References

[1] N. J. Gimsing and C. T. Georgakis, *Cable Supported Bridges: Concept and Design*, John Wiley & Sons, Chichester, UK, 3rd ed edition, 2011.

[2] Y. Deng, Y. Liu, and S. Chen, "Long-term in-service monitoring and performance assessment of the main cables of long-span suspension bridges," *Sensors*, vol. 17, no. 6, p. 1414, 2017.

[3] S. Cho, H. Jo, S. Jang et al., "Structural health monitoring of a cable-stayed bridge using wireless smart sensor technology: data analyses," *Smart Structures and Systems*, vol. 6, no. 5_6, pp. 461–480, 2010.

[4] D. A. Khazem, H. Kwun, S.-y. Kim, and C. Dynes, "Long-range inspection of suspender ropes in suspension bridges using the magnetostrictive sensor technology," in *Proceedings of the 3rd International Workshop on Structural Health Monitoring: The Demands and Challenges, 2001*, 2001, Citeseer.

[5] J. Xu, X. Wu, L. Wang, C. Huang, and Y. Kang, "Detecting the flaws in prestressing strands using guided waves based on the magnetostrictive effect," *Insight-Non-Destructive Testing and Condition Monitoring*, vol. 49, no. 11, pp. 647–650, 2007.

[6] C. Schaal, S. Bischoff, and L. Gaul, "Damage detection in multi-wire cables using guided ultrasonic waves," *Structural Health Monitoring*, vol. 15, no. 3, pp. 279–288, 2016.

[7] J. Xu, X. Wu, C. Cheng, and A. Ben, "A magnetic flux leakage and magnetostrictive guided wave hybrid transducer for detecting bridge cables," *Sensors*, vol. 12, no. 1, pp. 518–533, 2012.

[8] R. Raišutis, R. Kažys, L. Mažeika, E. Žukauskas, V. Samaitis, and A. Jankauskas, "Ultrasonic guided wave-based testing technique for inspection of multi-wire rope structures," *NDT & E International*, vol. 62, pp. 40–49, 2014.

[9] R. Ribichini, F. Cegla, P. B. Nagy, and P. Cawley, "Experimental and numerical evaluation of electromagnetic acoustic transducer performance on steel materials," *NDT & E International*, vol. 45, no. 1, pp. 32–38, 2012.

[10] H. Kwun, K. A. Bartels, and J. J. Hanley, "Effects of tensile loading on the properties of elastic-wave propagation in a strand," *The Journal of the Acoustical Society of America*, vol. 103, no. 6, pp. 3370–3375, 1998.

[11] B. Arturo, C. D. Hernandezsalazar, and B. Manzanaresmartinez, "Study of wave propagation in a multiwire cable to determine structural damage," *NDT and E International*, vol. 43, no. 8, pp. 726–732, 2010.

[12] J. Xu, X. J. Wu, and P. F. Sun, "Detecting broken-wire flaws at multiple locations in the same wire of prestressing strands using guided waves," *Ultrasonics*, vol. 53, no. 1, pp. 150–156, 2013.

[13] S. Chaki and G. Bourse, "Guided ultrasonic waves for non-destructive monitoring of the stress levels in prestressed steel strands," *Ultrasonics*, vol. 49, no. 2, pp. 162–171, 2009.

[14] S. Chaki and G. Bourse, "Stress level measurement in prestressed steel strands using acoustoelastic effect," *Experimental Mechanics*, vol. 49, no. 5, pp. 673–681, 2009.

[15] F. Treyssede, "Dispersion curve veering of longitudinal guided waves propagating inside prestressed seven-wire strands," *Journal of Sound and Vibration*, vol. 367, pp. 56–68, 2016.

[16] F. Treyssède, "Investigation of the interwire energy transfer of elastic guided waves inside prestressed cables," *The Journal of the Acoustical Society of America*, vol. 140, no. 1, pp. 498–509, 2016.

[17] X. Liu, B. Wu, F. Qin, C. He, and Q. Han, "Observation of ultrasonic guided wave propagation behaviours in pre-stressed multi-wire structures," *Ultrasonics*, vol. 73, pp. 196–205, 2017.

[18] B. Dubuc, A. Ebrahimkhanlou, and S. Salamone, "Higher order longitudinal guided wave modes in axially stressed seven-wire strands," *Ultrasonics*, vol. 84, pp. 382–391, 2018.

[19] D. C. Jiles, "Theory of the magnetomechanical effect," *Journal of Physics D: Applied Physics*, vol. 28, no. 8, pp. 1537–1546, 1995.

[20] M. J. Sablik, K. L. Telschow, B. Augustyniak, J. Grubba, and M. Chmielewski, "Relationship between magnetostriction and the magnetostrictive coupling coefficient for magnetostrictive generation of elastic waves," in *AIP Conference Proceedings*, pp. 1613–1620, Brunswick, ME, USA, 2002.

[21] M. J. Sablik, H. Kwun, G. L. Burkhardt, and D. C. Jiles, "Model for the effect of tensile and compressive stress on ferromagnetic hysteresis," *Journal of Applied Physics*, vol. 61, no. 8, pp. 3799–3801, 1987.

[22] M. Roskosz and M. Bieniek, "Evaluation of residual stress in ferromagnetic steels based on residual magnetic field measurements," *NDT and E International*, vol. 45, no. 1, pp. 55–62, 2012.

[23] F. Lanza di Scalea, P. Rizzo, and F. Seible, "Stress measurement and defect detection in steel strands by guided stress waves," *Journal of Materials in Civil Engineering*, vol. 15, no. 3, pp. 219–227, 2003.

[24] P. Rizzo and F. L. Di Scalea, "Load measurement and health monitoring in cable stays via guided wave magnetostrictive ultrasonics," *Materials Evaluation*, vol. 62, pp. 1057–1065, 2004.

[25] P. Rizzo, "Ultrasonic wave propagation in progressively loaded multi-wire strands," *Experimental Mechanics*, vol. 46, no. 3, pp. 297–306, 2006.

[26] M. J. Sablik and S. W. Rubin, "Modeling magnetostrictive generation of elastic waves in steel pipes, I. Theory," *International Journal of Applied Electromagnetics and Mechanics*, vol. 10, no. 2, pp. 143–166, 1999.

[27] M. J. Sablik, Y. Lu, and G. L. Burkhardt, "Modeling magnetostrictive generation of elastic waves in steel pipes, II. Comparison to experiment," *International Journal of Applied Electromagnetics and Mechanics*, vol. 10, no. 2, pp. 167–176, 1999.

[28] X. Song, Z. Jin, and H. Yu, "Influences of magnetic circuit structure of magnetostrictive guided wave transducer on the homogeneity of bias magnetic field," *International Journal of Applied Electromagnetics and Mechanics*, vol. 33, no. 2, pp. 581–588, 2010.

[29] W. Kim and Y. Y. Kim, "Design of a bias magnetic system of a magnetostrictive sensor for flexural wave measurement," *IEEE Transactions on Magnetics*, vol. 40, no. 5, pp. 3331–3338, 2004.

[30] S. Gurevich, "The theory of electromagnetic generation of acoustic waves in a ferromagnetic medium at a high temperature," *Russian Journal of Nondestructive Testing*, vol. 29, pp. 193–204, 1993.

[31] M. J. Sablik, G. L. Burkhardt, H. Kwun, and D. C. Jiles, "A model for the effect of stress on the low-frequency harmonic content of the magnetic induction in ferromagnetic materials," *Journal of Applied Physics*, vol. 63, no. 8, pp. 3930–3932, 1988.

[32] M. J. Sablik, T. Yonamine, and F. J. G. Landgraf, "Modeling plastic deformation effects in steel on hysteresis loops with the same maximum flux density," *IEEE Transactions on Magnetics*, vol. 40, no. 5, pp. 3219–3226, 2004.

[33] M. J. Sablik and D. C. Jiles, "Coupled magnetoelastic theory of magnetic and magnetostrictive hysteresis," *IEEE Transactions on Magnetics*, vol. 29, no. 4, pp. 2113–2123, 1993.